

# The influence of particle composition on thorium scavenging in the NE Atlantic ocean (POMME experiment)

M. Roy-Barman <sup>a,\*</sup>, C. Jeandel <sup>b</sup>, M. Souhaut <sup>b</sup>, M. Rutgers van der Loeff <sup>c</sup>,  
I. Voege <sup>c</sup>, N. Leblond <sup>d</sup>, R. Freydier <sup>e</sup>

<sup>a</sup> *Laboratoire des Sciences du Climat et de l'Environnement/Institut Pierre Simon Laplace, CNRS, 91198 Gif-sur-Yvette Cedex, France*

<sup>b</sup> *LEGOS (CNRS/CNES/IRD/UPS), Observatoire Midi-Pyrénées, 14, Av. E. Belin, 31400 Toulouse, France*

<sup>c</sup> *AWI, PO Box 120161, 27515 Bremerhaven, Germany*

<sup>d</sup> *Laboratoire d'Océanographie de Villefranche, La Darse, BP 08, 06238 Villefranche-sur-mer, Cedex, France*

<sup>e</sup> *LMTG, Observatoire Midi-Pyrénées, 14, Av. E. Belin, 31400 Toulouse, France*

Received 8 February 2005; received in revised form 22 September 2005; accepted 22 September 2005

Available online 10 November 2005

Editor: E. Boyle

## Abstract

<sup>230</sup>Th, <sup>232</sup>Th and <sup>234</sup>Th were analyzed in sinking particles collected by moored and drifting sediment traps in the NE Atlantic Ocean (POMME experiment) in order to constrain the phase(s) carrying Th isotopes in the water column. It reveals a contrasted behaviour between <sup>234</sup>Th and <sup>230</sup>Th. <sup>234</sup>Th is correlated to the particulate organic carbon suggesting that it is primarily scavenged by organic compounds in the surface waters. <sup>230</sup>Th<sub>xs</sub> is correlated with Mn, Ba and the lithogenic fraction that are enriched in small suspended particles and incorporated in the sinking particulate flux throughout the water column. The lack of correlation between <sup>230</sup>Th<sub>xs</sub> and CaCO<sub>3</sub> or biogenic silica (bSi) indicates that CaCO<sub>3</sub> and bSi are not responsible for <sup>230</sup>Th scavenging in the deep waters of this oceanic region. <sup>230</sup>Th is generally correlated with the lithogenic content of the trapped material but this correlation disappears in winter during strong atmospheric dust inputs suggesting that lithogenic matter is not directly responsible for <sup>230</sup>Th scavenging in the deep waters or that sufficient time is required to achieve particle–solution equilibration. MnO<sub>2</sub> could be the prevalent <sup>230</sup>Th<sub>xs</sub>-bearing phase. The narrow range of  $K_{d\_MnO_2}^{Th}$  obtained for very contrasted oceanic environments supports a global control of <sup>230</sup>Th<sub>xs</sub> scavenging by MnO<sub>2</sub> and raises the possibility that the <sup>230</sup>Th–<sup>231</sup>Pa fractionation is controlled by the amount of colloidal MnO<sub>2</sub> in seawater.

© 2005 Elsevier B.V. All rights reserved.

**Keywords:** thorium isotopes; seawater; marine particles; manganese oxides; Atlantic

## 1. Introduction

Understanding the oceanic carbon cycle requires reliable estimates of the particulate carbon fluxes from the surface waters to the bottom of the ocean. Particulate

fluxes are usually measured with sediment traps. Unfortunately, turbulence around the aperture of the trap can prevent a significant fraction of the sinking particles from being collected [1]. Therefore, it is necessary to evaluate the sediment trap efficiency. Thorium isotopes are used to perform this evaluation [2,3]. <sup>230</sup>Th and <sup>234</sup>Th are produced uniformly in the ocean by radioactive decay of Uranium isotopes (<sup>234</sup>U and <sup>238</sup>U). Because thorium is a very particle-reactive element, Th isotopes

\* Corresponding author. Tel.: +33 1 69 82 35 66; fax: +33 1 69 82 35 68.  
E-mail address: [Matthieu.Roy-Barman@lsce.cnrs-gif.fr](mailto:Matthieu.Roy-Barman@lsce.cnrs-gif.fr)  
(M. Roy-Barman).

are rapidly scavenged on sinking particles and transported towards the bottom of the ocean [4]. The theoretical flux of Th carried by sinking particles is calculated as the difference between radioactive production and radioactive decay in the water column above the trap. The trapping efficiency is the ratio between the trapped flux and the calculated one. Trapping efficiencies as low as 10% are obtained in the surface waters and in the mesopelagic zone (where horizontal currents are high) confirming that some traps largely undercollect the particle flux [5]. Sediment trap may also discriminate among different types of particles: large and rapidly sinking particles are expected to be collected more efficiently than small and slowly sinking particles [6]. Therefore, a Th-based trapping efficiency may not be relevant for all particles and compounds collected by the traps. Using or ignoring trapping efficiency corrections lead to very different pictures of the particle flux evolution throughout the water column indeed [5,7]. Thus, the determination of the phase(s) carrying Th isotopes is a key issue.

At present, there is no consensus on the question. The common idea that “Th probably sticks identically on all types of particles” relies on the gross correlation between the fluxes of Th and of the major phases in the traps [5]. However, it is not supported by detailed studies of the partition coefficient  $K_{d,bulk}^{Th}$  between the bulk particulate and the dissolved phases (field-based estimate of  $K_{d,bulk}^{Th}$  is obtained by dividing the amount of nuclides per g of bulk trapped particles by the total amount of nuclides (dissolved+particulate) per g of seawater in the water through which the particle sunk). In the southern and Pacific oceans, the correlation between  $K_{d,bulk}^{Th}$  and the carbonate content of trapped particles suggests that  $^{230}Th$  scavenging is controlled by carbonates [8]. In regions with higher lithogenic content in the trapped material, both carbonate and lithogenic material should scavenge  $^{230}Th$  [8,9]. Revisiting the same data set, Luo and Ku (2004) noted a strong correlation between  $K_{d,bulk}^{Th}$  and the lithogenic content of the trapped particles and proposed that  $^{230}Th$  is scavenged mainly by the lithogenic phase [10,11]. In fact, that particular set of samples does not allow to decide conclusively which of the 2 phases scavenges  $^{230}Th$  because the lithogenic content, the carbonate content and the  $K_{d,bulk}^{Th}$  are correlated. In the Arctic Ocean where biological productivity is very low, ice-rafterd lithogenic particles are proposed to scavenge  $^{230}Th$  [12–14]. Independently of the  $^{230}Th$  works, numerous studies of  $^{234}Th$  export from the surface ocean have led to the conclusion that  $^{234}Th$  is primarily scavenged by organic colloids [15], although the lithogenic phase might play a significant role in the coastal and

high dust regions [16]. It seems difficult to draw a clear picture from all these studies as they produced either competing or contradictory conclusions. In addition,  $^{234}Th$  and  $^{230}Th$  are often measured with different background parameters because of their distinct applications, so that the different studies cannot be compared easily.

Here we present a coherent set of sediment trap data obtained during the POMME (Programme Océan Multidisciplinaire Méso Echelle or MesoScale Multidisciplinary Ocean Program) experiment in the NE Atlantic Ocean that allows the direct comparison of  $^{230}Th$ ,  $^{232}Th$ ,  $^{234}Th$  and of the main components of the trapped particles. The general setting and the goals of the POMME program are described elsewhere [17]. During the POMME program, the sinking particles were collected with both long-term moorings and drifting sediment traps deployed for a few days at different seasons. This combination of traps allowed to measure and compare  $^{230}Th$ ,  $^{232}Th$  (moorings) and  $^{234}Th$ ,  $^{232}Th$  (drifting traps) in the same oceanographic setting.

## 2. Sampling and analytical methods

### 2.1. Trap deployment

All the traps used during POMME were multisampling conical sediment-traps (PPS5) with a collection surface of 1 m<sup>2</sup>. All the sampling cups were poisoned with formaldehyde prior to trap deployment in order to prevent feeding in the traps. We report the results obtained on Southwest (39°34.85N, 18°51.23W, water depth: 4786 m) and Northeast moorings (43°32.867N, 17°20.868W, water depth: 3760 m) of POMME (hereafter SW and NE moorings). Moored sediment traps were deployed at 400 and 1000 m over two periods: all the traps were deployed from February 2001 to August 2001 (sampling interval=8 days) and the NE traps were deployed again from August 2001 to June 2002 (sampling interval=12 days). We also report results obtained with drifting sediment traps deployed at 400 m during the POMME experiment in winter (POMME 1), spring (POMME 2) and end of summer (POMME 3) 2001. Drifting traps were deployed at 400 m for 48 h during long stations occupied over the POMME area (between 39–43°N and 17–19°W). Detailed location of the traps can be found in [18,19].

### 2.2. Analysis of the major phases

Sampling procedures followed the JGOFS protocols and can be found at <http://www.obs-vlfr.fr/LOV/Pieges/>. Back in the laboratory, swimmers were removed from

the samples. The whole sample was then rinsed with ultra-pure water (MilliQ) and freeze-dried. Concentrations of Total Carbon (TC) carbon were measured in triplicate with a LECO 900 elemental analyzer (CHN) on aliquots of the desiccated samples. Acid ( $\text{HNO}_3 + \text{HF}$ ) digestions in microwave oven were performed on 20 mg aliquots of the desiccated samples. For all the acid-digested samples, Al, Fe, and Ca were analyzed by ICP/AES (Jobin Yvon JY 138 'Ultra', LOV, Villefranche sur mer), whereas  $^{232}\text{Th}$ , Ba, Mn and Rare Earth Elements (REE) were analyzed by ICP/MS (Perkin Elmer Elan 6000, LEGOS, Toulouse). The detailed procedures as well as their validation are given in [19].

### 2.3. Analysis of $^{230}\text{Th}$ and $^{232}\text{Th}$

$^{230}\text{Th}$  and  $^{232}\text{Th}$  were analyzed on the samples collected by the moored sediment traps on an aliquot of the solution obtained for major and trace elements (see above).  $^{229}\text{Th}$  spike was added to this aliquot. After isotopic equilibration, the Th was purified by ion exchange chemistry [20]. Procedural blanks (around 20 pg of  $^{232}\text{Th}$  and 0.1 fg of  $^{230}\text{Th}$ ) represent typically less than 1–2% of the Th in the samples. For the SW400 and SW1000 traps and the first period of the NW400 trap, the purified Th was analyzed by TIMS on a Finnigan Mat 262 mass spectrometer as described in [21]. The remaining samples (the second period of the NE400 trap and the two periods of the NE1000 trap) were analyzed in Toulouse by MC-ICP-MS on a Neptune (Finnigan) instrument. The detailed procedure will be published elsewhere. There is an excellent agreement between the TIMS and MC-ICP-MS measurements (Fig. 1). Note that  $^{232}\text{Th}$  was also determined on all samples by quadrupole ICP-MS (Perkin Elmer Elan 6000, LEGOS, Toulouse). There is an excellent agreement ( $r^2 > 0.985$ ) between the determinations of  $^{232}\text{Th}$  by the 3 methods (TIMS, quadrupole ICP-MS and MC-ICPMS).  $^{232}\text{Th}$  data obtained by quadrupole ICP-MS are used only for the drifting traps that were not analyzed for  $^{230}\text{Th}$ .

### 2.4. Analysis of $^{234}\text{Th}$

$^{234}\text{Th}$  was analyzed on the samples collected by the drifting traps. Compared to  $^{230}\text{Th}$ , a shorter procedure was used due to the short half-life of  $^{234}\text{Th}$ . For each trap, an aliquot of each cup was collected before the swimmer removal and these aliquots were put together in order to obtain sufficient  $^{234}\text{Th}$  activities. All samples were analyzed by gamma counting in a well-type low-background detector [22]. It can be noted that  $^{234}\text{Th}$  was not analyzed on the same aliquots than major and

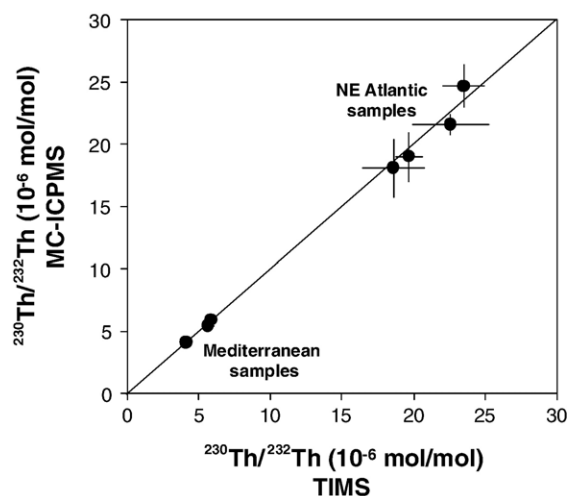


Fig. 1. Comparison of TIMS and MC-ICP-MS analysis of sediment trap samples. For each sample, both measurements correspond to aliquots of the same solution obtained after the ion exchange chemistry. These aliquots contained  $\sim 0.4$  ng of  $^{232}\text{Th}$  and  $\sim 8$  fg of  $^{230}\text{Th}$  for the NE Atlantic (NE400) samples and  $\sim 5$  ng of  $^{232}\text{Th}$  and  $\sim 25$  fg of  $^{230}\text{Th}$  for the Mediterranean samples.

trace elements. Major and trace elements were analyzed on each cup after the swimmer removal with the procedure used for the moored traps. Concentrations averaged over the whole collection period have been recalculated for comparison with  $^{234}\text{Th}$  data.

## 3. Results

Thorium isotopes and Mn data are available in electronic form (see Appendix 1–5 in the *Background data set*). All major element and Ba data are available at (<http://www.lodyc.jussieu.fr/POMME/>). Detailed composition of the material collected by moored and drifting traps are given in [18,19]. The material collected by the traps is made of fecal pellets, marine snow and individual foraminifera tests in variable proportions. In the following, we will focus on the relationship between Th isotopes and the abundance of different phases such as calcium carbonate, biogenic silica (bSi), organic matter, and lithogenic material. Unlike  $^{230}\text{Th}$  and  $^{234}\text{Th}$ ,  $^{232}\text{Th}$  is not produced in situ but only brought to the ocean by lithogenic particles. Assuming that all the  $^{232}\text{Th}$  is carried by lithogenic particles [23] and that the  $^{232}\text{Th}$  concentration in these particles is 10 ppm [24], the lithogenic fraction is given by  $\% \text{Litho} = 0.1 \times ^{232}\text{Th}$  (in ppm). The carbonate fraction was determined from particulate Ca concentrations as follows:  $\% \text{CaCO}_3 = 2.5 \times \% \text{Ca}$ . Particulate Inorganic Carbon (PIC) was calculated as  $\% \text{PIC} = \% \text{CaCO}_3 / 8.33$ . The Particulate Organic Carbon (POC) was cal-

culated as the difference between TC and PIC. The organic matter content is about twice the POC content. Biogenic silica ( $\text{SiO}_2, n\text{H}_2\text{O}$ ), was calculated assuming  $n=0.4$  [25]. It represents less than 30% of the trapped material [26,27]. Excess Ba ( $\text{Ba}_{\text{XS}}$ ) was used to evaluate the abundance of biogenic Ba [19]. It was calculated as the bulk Ba content corrected from the terrigenous Ba contribution. Terrigenous Ba is estimated using a reference crustal  $\text{Ba}/^{232}\text{Th}$  ratio, applying a crustal  $\text{Ba}/^{232}\text{Th}$  (wt/wt) ratio of 51.4 [24]. Mn was measured to evaluate the abundance of Mn oxides.

The  $^{230}\text{Th}$  produced by in situ decay of dissolved  $^{234}\text{U}$  and that is scavenged on particles ( $^{230}\text{Th}_{\text{XS}}$ ) is calculated by subtracting the lithogenic  $^{230}\text{Th}$  component to the total  $^{230}\text{Th}$ :

$$^{230}\text{Th}_{\text{XS}} = ^{230}\text{Th}_{\text{measured}} - ^{232}\text{Th}_{\text{measured}} \times (^{230}\text{Th}/^{232}\text{Th})_{\text{litho}} \quad (1)$$

with  $(^{230}\text{Th}/^{232}\text{Th})_{\text{litho}} = 4.4 \times 10^{-6}$  mol/mol based on a mean composition of the continental crust [28]. The  $^{230}\text{Th}_{\text{XS}}$  concentrations range from 0.3 to 10.7 pg/g at 400 m and from 1.8 to 27 pg/g at 1000 m (Fig. 2). The

highest  $^{230}\text{Th}_{\text{XS}}$  concentrations are generally found in the deepest traps and from summer to winter whereas the  $^{230}\text{Th}_{\text{XS}}$  concentrations are low during the spring bloom. In the NE traps, low  $^{230}\text{Th}_{\text{XS}}$  concentrations are found until August because the biologically productive period was longer due to the occurrence of short wind events that deepened the mixed layer as well as to the meso-scale activity [19]. During POMME,  $^{230}\text{Th}_{\text{XS}}$  represents more than 75% of the total  $^{230}\text{Th}$ , except during the high dust event recorded by the SW traps when  $^{230}\text{Th}_{\text{XS}}$  represents  $\sim 50\%$  of the total  $^{230}\text{Th}$ . For the moored trap samples, there is no correlation between  $^{230}\text{Th}_{\text{XS}}$  and  $\text{CaCO}_3$  (NE400:  $r^2=0.16$ , NE1000:  $r^2=0.0006$ , SW400:  $r^2=0.001$ , SW1000:  $r^2=0.11$ ) or POC (NE400:  $r^2=0.22$ , NE1000:  $r^2=0.01$ , SW400:  $r^2=0.21$ , SW1000:  $r^2=0.04$ ) or bSi in general (NE400:  $r^2=0.57$ , NE1000:  $r^2=0.02$ , SW400:  $r^2=0.01$ , SW1000:  $r^2=0.001$ ) (Fig. 3a–c). Conversely, there are correlations between  $^{230}\text{Th}_{\text{XS}}$  and Mn (NE400:  $r^2=0.47$ , NE1000:  $r^2=0.89$ , SW400:  $r^2=0.75$ , SW1000:  $r^2=0.90$ ) or Ba (NE400:  $r^2=0.63$ , NE1000:  $r^2=0.90$ , SW400:  $r^2=0.80$ , SW1000:  $r^2=0.77$ ) (Fig. 3d–f). In the case of Mn or Ba, distinct correlations with  $^{230}\text{Th}_{\text{XS}}$  are obtained at 400 m and

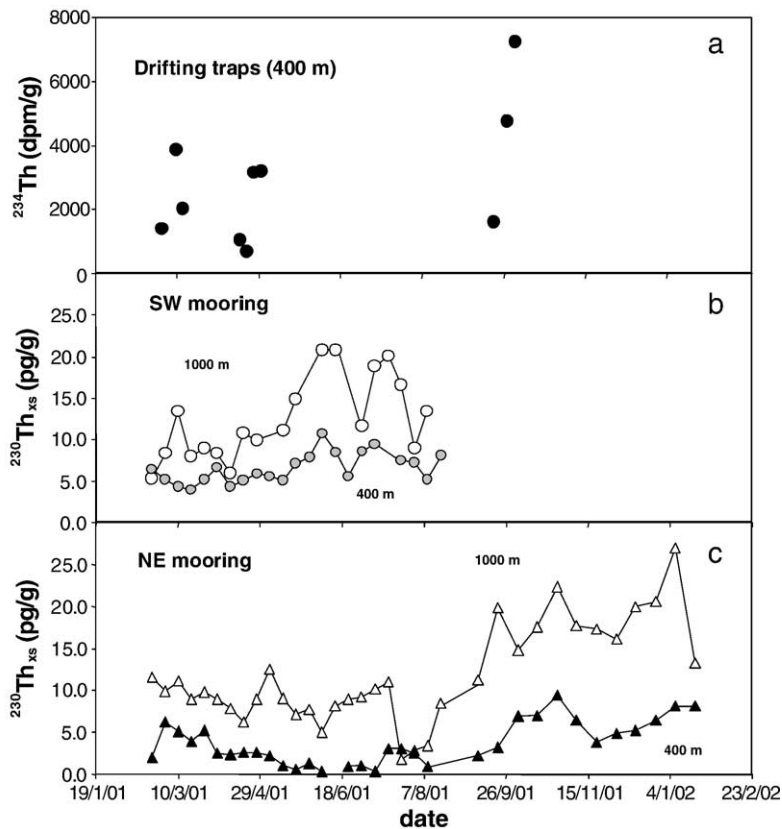


Fig. 2. Temporal evolution of  $^{230}\text{Th}_{\text{XS}}$  and  $^{234}\text{Th}$  in the trapped particles. (a)  $^{230}\text{Th}_{\text{XS}}$  at the NE mooring. (b)  $^{230}\text{Th}_{\text{XS}}$  at the SW mooring. (c)  $^{234}\text{Th}$  in the drifting traps (400 m).

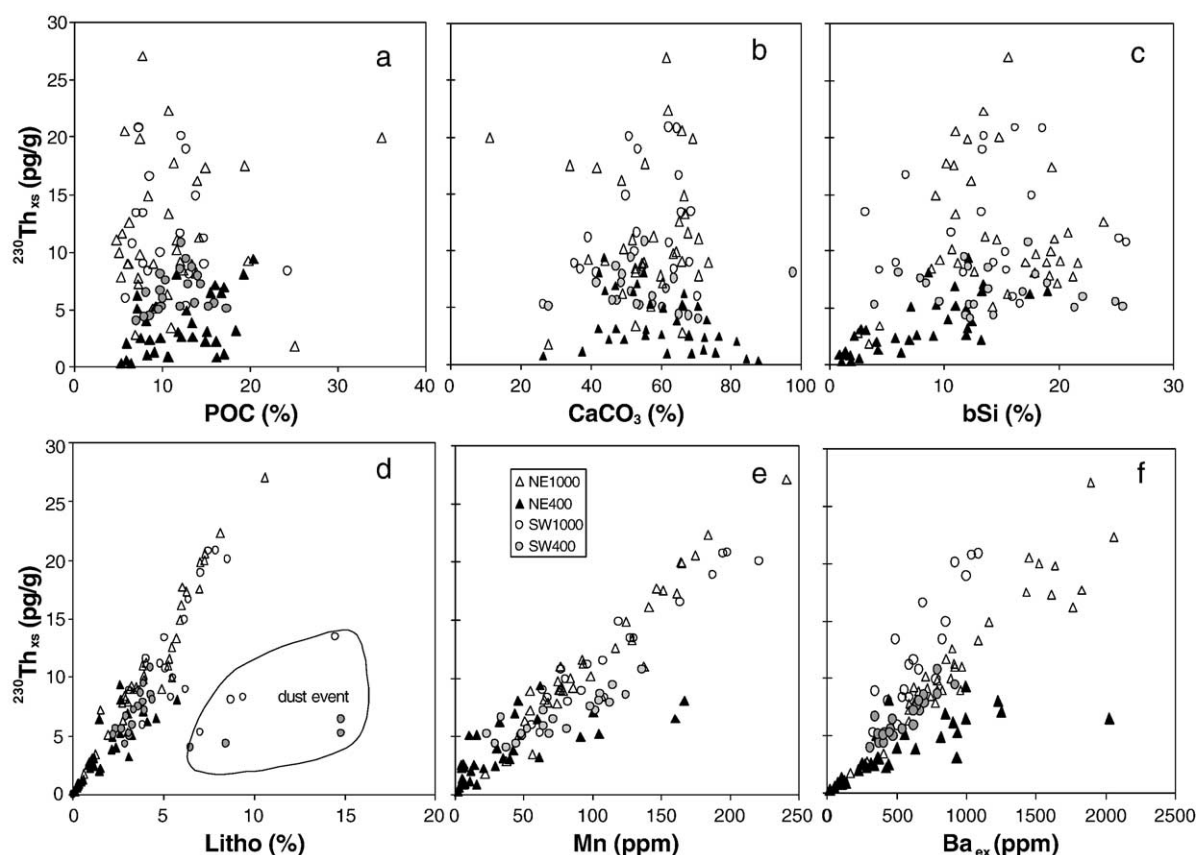


Fig. 3.  $^{230}\text{Th}_{\text{xs}}$  as a function of the particle composition. (a)  $^{230}\text{Th}_{\text{xs}}$  versus POC. (b)  $^{230}\text{Th}_{\text{xs}}$  versus  $\text{CaCO}_3$ . (c)  $^{230}\text{Th}_{\text{xs}}$  versus biogenic silica. (d)  $^{230}\text{Th}_{\text{xs}}$  versus lithogenic fraction. (e)  $^{230}\text{Th}_{\text{xs}}$  versus Mn. (f)  $^{230}\text{Th}_{\text{xs}}$  versus  $\text{Ba}_{\text{ex}}$ .

1000 m due to the enrichment of  $^{230}\text{Th}_{\text{xs}}$  on marine particles with depth. Except for a few samples (8 out of 100) from the SW traps, there is a good correlation between the lithogenic content and  $^{230}\text{Th}_{\text{xs}}$  that holds both at 400 m and 1000 m (NE400:  $r^2=0.75$ , NE1000:  $r^2=0.93$ , SW400:  $r^2=0.69$  (excluding the 4 high dust samples), SW1000:  $r^2=0.69$  (excluding the 4 high dust samples)).

The particles collected by the drifting traps have  $^{234}\text{Th}$  activities ranging from 661 to 7206 dpm/g. There is a positive correlation between  $^{234}\text{Th}$  and POC ( $r^2=0.67$ ) and no significant correlation between  $^{234}\text{Th}$  and  $\text{CaCO}_3$  ( $r^2=0.01$ ), the lithogenic fraction ( $r^2=0.01$ ), bSi ( $r^2=0.07$ ), Mn ( $r^2=0.02$ ) or Ba ( $r^2=0.01$ ) (Fig. 4a–e). The POC/ $^{234}\text{Th}$  ratio range from 1.1 to 6.0  $\mu\text{mol}/\text{dpm}$ .

## 4. Discussion

### 4.1. Testing the role of the major phases

In the following discussion, we will compare samples collected at different sites and depths with drifting

or moored traps. During the POMME program, the spatial variability of the particle flux (related to a North–South gradient of mixed layer depth and to mesoscale structures) is much smaller than the seasonal variability occurring all over the POMME area [19]. Therefore, it makes sense to compare the material collected by drifting and traps over the POMME area. In addition, conical traps are known to under-collect particles, especially in high-energy shallow water. This may affect the composition of particles collected by drifting versus moored traps or by shallow versus deep traps. These traps do not necessarily collect the same types of particles because they experience different shearing flows that do not generate the same turbulence around and in the traps. However, the similar ranges of major and trace element found in the material collected by the different traps suggest that all the traps generally collect similar particles.

The correlations presented in the previous section suggest that trapped particles are a mixture of 2 components [2,29]: (1) small suspended particles with high content of  $^{230}\text{Th}$ , the lithogenic material, Ba, Mn and

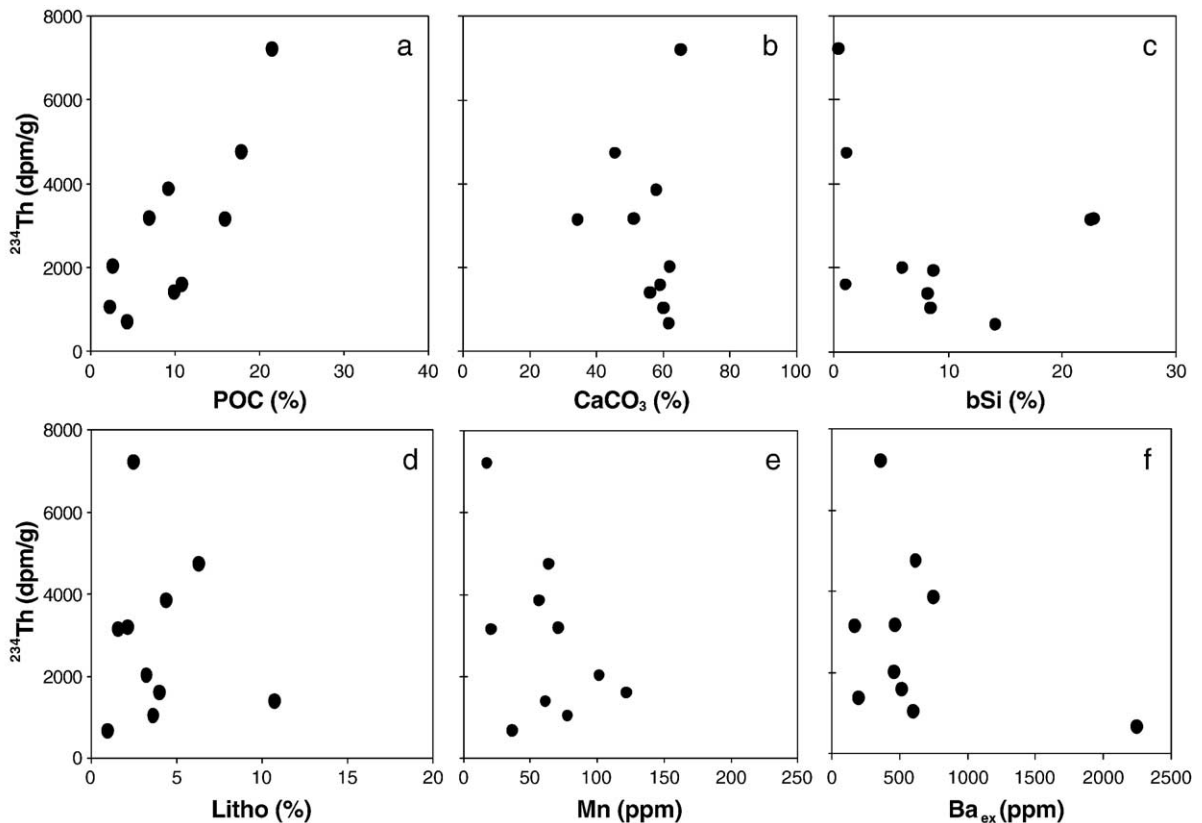


Fig. 4.  $^{234}\text{Th}$  as a function of the particle composition. (a)  $^{234}\text{Th}$  versus POC. (b)  $^{234}\text{Th}$  versus  $\text{CaCO}_3$ . (c)  $^{234}\text{Th}$  versus biogenic silica. (d)  $^{234}\text{Th}$  versus lithogenic material. (e)  $^{234}\text{Th}$  versus Mn. (f)  $^{234}\text{Th}$  versus  $\text{Ba}_{\text{ex}}$ .

(2) fresh particles recently produced in the surface waters that contain little  $^{230}\text{Th}$ , Mn, Ba or lithogenic material but that have high content in POC,  $^{234}\text{Th}$  and  $\text{CaCO}_3$ . The correlation between  $^{230}\text{Th}$  and the lithogenic fraction, Ba or Mn reflects the dilution of the small particles by a variable amount of newly surface derived material (aggregation of suspended particles on the sinking particles).

As noted previously, a correlation between  $^{230}\text{Th}_{\text{XS}}$  and a given phase does not imply that this phase carries  $^{230}\text{Th}_{\text{XS}}$ . It is best illustrated by the  $^{230}\text{Th}_{\text{XS}}-\text{Ba}_{\text{XS}}$  case (Fig. 3f).  $^{230}\text{Th}_{\text{XS}}$  and  $\text{Ba}_{\text{XS}}$  are correlated in the trapped particles because they are both aggregated from the small particle pool. In the mesopelagic zone, particulate  $\text{Ba}_{\text{XS}}$  is located quantitatively in barite crystals ( $\text{BaSO}_4$ ) [30,31]. The remaining particulate Ba is found in the lithogenic phase and represents usually less than 10% of the total Ba in the POMME area [19]. Carbonates are not a significant host for Ba [32]. The  $^{230}\text{Th}_{\text{XS}}$  content of barite in marine sediments varies from 0 to 200 pg/g for water depths ranging from 2000 m to 4600 m [33]. Taken on face value, if barite in the POMME samples had a  $^{230}\text{Th}_{\text{XS}}$  concentration of 200 pg/g, it would

account for 3–26% of the  $^{230}\text{Th}_{\text{XS}}$  in the trapped material. However,  $^{230}\text{Th}_{\text{XS}}$ -rich barite are extracted from sediments located below the lysocline so that the  $^{230}\text{Th}_{\text{XS}}$  enrichment could be due to sediment dissolution. On the contrary, in sediments located above the lysocline, barite contains no  $^{230}\text{Th}_{\text{XS}}$  and could not contribute significantly to the  $^{230}\text{Th}_{\text{XS}}$  content of the trapped material. Therefore, Barite probably does not contain a large fraction of the  $^{230}\text{Th}$  despite the significant  $\text{Ba}_{\text{XS}}-^{230}\text{Th}_{\text{XS}}$  correlation.

The lack of correlation between  $^{234}\text{Th}$  and bSi in the drifting traps and between  $^{230}\text{Th}_{\text{XS}}$  and bSi in NE100, SW1000 and SW400 suggests that bSi is not the main  $^{230}\text{Th}$  carrier in the POMME samples (Fig. 3c). This is consistent with results from the Southern Ocean and the Equatorial Pacific where inverse correlations between  $^{230}\text{Th}_{\text{XS}}$  and bSi imply that  $^{230}\text{Th}$  has a lower affinity for bSi than for other phases constituting the trapped material [8]. The correlation between  $^{230}\text{Th}_{\text{XS}}$  and bSi at NE400 seems spurious (particularly if we consider the lack of correlation for the other traps): It is mainly driven by samples with low bSi and small particles (enriched in lithogenic, Mn and  $^{230}\text{Th}_{\text{XS}}$ ) content col-

lected by this trap. It may be due to a low trapping efficiency [19] compared to carbonate-rich particles.

The lack of correlation between  $^{230}\text{Th}_{\text{xs}}$  and  $\text{CaCO}_3$  (Fig. 3b) suggests that  $\text{CaCO}_3$  is not an important  $^{230}\text{Th}$  carrier in the POMME samples. This seems to contradict data obtained in the Southern Ocean and the Equatorial Pacific where the strong correlation between  $^{230}\text{Th}_{\text{xs}}$ – $\text{CaCO}_3$  was used to infer that  $\text{CaCO}_3$  could be an important  $^{230}\text{Th}_{\text{xs}}$  carrier at least for samples containing less than 5% of lithogenic fraction [8]. Considering only the POMME samples with less than 5% of lithogenic fraction (this is the case of all the NE400 samples on Fig. 3b) does not reveal a correlation between  $\text{CaCO}_3$  and  $^{230}\text{Th}_{\text{xs}}$ . This may be due to the high foraminifera content of many POMME samples, because foraminifera may sink too rapidly to scavenge  $^{230}\text{Th}$ . However, even if we just consider samples with less than 5% of lithogenic fraction and less than 10% of foraminifera (visual estimate of the volume of foraminifera tests compared to faecal pellets and marine snow), there is still no correlation between  $^{230}\text{Th}_{\text{xs}}$  and the  $\text{CaCO}_3$  (for 8 samples,  $r^2=0.0004$ , figure not shown). As a consequence, we conclude that  $\text{CaCO}_3$  is not the main  $^{230}\text{Th}_{\text{xs}}$  carrier in the POMME area. The  $^{230}\text{Th}$ – $\text{CaCO}_3$  correlations observed in the Southern Ocean and in the equatorial Pacific might be spurious [8]. In the Southern Ocean and in the equatorial Pacific, diatoms dominate the primary production, so that fresh marine particles are rich in bSi. It is well established that seawater is undersaturated with respect to bSi throughout the water column, whereas  $\text{CaCO}_3$  remains stable over much of the water column and that the lithogenic fraction is expected to experience little (if any) dissolution. The high dissolution rate of bSi [34] accounts for the sharp decrease of the bSi concentration with depth in the water column of the southern ocean whereas the lithogenic silica concentration remains fairly constant [35]. Similarly, the bSi/ $\text{CaCO}_3$  ratio in the small particle pool decreases with depth due to a preferential dissolution of diatoms test compared to carbonates and/or a preferential accumulation of coccolithophorids (and lithogenic particles) compared to diatoms in the small particle pool [36]. Therefore, in the deep waters, the small particles pool is enriched in  $\text{CaCO}_3$  and lithogenic particles compared to bSi and it is also enriched in  $^{230}\text{Th}_{\text{xs}}$  [4] because  $^{230}\text{Th}_{\text{xs}}$  increases with depth by reversible scavenging whatever the real Th bearing phases are. Conversely, large sinking particles freshly produced in the surface waters are bSi-rich and  $^{230}\text{Th}_{\text{xs}}$ -poor because there is little  $^{230}\text{Th}_{\text{xs}}$  to scavenge in the shallow water. Finally, aggregation of small particles

(enriched simultaneously in  $^{230}\text{Th}_{\text{xs}}$ ,  $\text{CaCO}_3$  and lithogenic matter) to the rapidly sinking particles (bSi-rich and  $^{230}\text{Th}_{\text{xs}}$ -poor) in the deep waters would produce the correlation between  $^{230}\text{Th}_{\text{xs}}$  and the  $\text{CaCO}_3$  fraction or the lithogenic fraction.

The lack of correlation between  $^{234}\text{Th}$  and  $\text{CaCO}_3$  strengthens the idea that calcium carbonate is not the main Th scavenging phase (at least in the surface waters). These results are consistent with the low value of  $K_{\text{d-CaCO}_3}^{\text{Th}}$  (the partition coefficient between pure  $\text{CaCO}_3$  and seawater) obtained by direct analysis of marine calcite samples [37] and by in vitro experiments [38]. These  $K_{\text{d-CaCO}_3}^{\text{Th}}$  (equal or less than  $5 \times 10^5$  ml/g) values are more than one order of magnitude lower than the value proposed by [8] based on sediment trap analysis ( $\approx 10^7$  ml/g).

The lack of correlation between  $^{230}\text{Th}_{\text{xs}}$  and POC in the moored trap samples (Fig. 3a) contrasts with the  $^{234}\text{Th}$ –POC correlation in the drifting trap samples (Fig. 4a). Although both isotopes are produced uniformly in the water column and have identical chemical properties, they experience different scavenging conditions with depth. With its short half-life,  $^{234}\text{Th}$  is most sensitive to the high scavenging rate in the surface waters due to the production of strong Th ligands by the biological activity, so that it is not surprising to find a  $^{234}\text{Th}$ –POC correlation. [15,39,40]. In the deeper water, the concentration of these ligands decreases rapidly [41], so that suspended particles contain little  $^{234}\text{Th}$  due to its lower scavenging rate and because  $^{234}\text{Th}$  is lost by radioactive decay. Conversely,  $^{230}\text{Th}$  accumulates on the particulate matter throughout the water column so that the contribution of surface derived  $^{230}\text{Th}$  is small at 400 m or 1000 m. While this differential behaviour of Th isotopes has been modelled [42], the present data provide a clear illustration of the model prediction.

There is not a simple correlation between  $^{230}\text{Th}_{\text{xs}}$  and the lithogenic fraction (Fig. 3d). For most samples, there is a good linear relationship between  $^{230}\text{Th}_{\text{xs}}$  and the lithogenic fraction indicating that they are both enriched in the small particles pool. Only the samples collected during February/March 2001 by the SW traps do not fall on the main trend (encircled in Fig. 4d). Their low Mn, Ba and  $^{230}\text{Th}$  contents indicate a low contribution of the small suspended particle pool despite a large lithogenic content. In the POMME area, the aeolian dust flux is generally low [43] but sporadic Saharan dust inputs occur. These samples were collected just after the arrival over the south of the POMME area of an aeolian dust plume recorded by satellite remote sensing on 13 February 2001 [26]. It appears

that this increase of lithogenic fraction in sinking particles by surface derived particles does not produce an increase of  $^{230}\text{Th}_{\text{xs}}$  concentration. The reason may be that the lithogenic material is not the main  $^{230}\text{Th}_{\text{xs}}$  carrier or that the lithogenic material locked inside the faecal pellets did not have opportunity or time to scavenge  $^{230}\text{Th}_{\text{xs}}$  (during February–March 2001 faecal pellets constituted most of the trapped material). In the SW traps, more than 50% of the total lithogenic flux was collected during the “high dust” event whereas only 30% of the  $^{230}\text{Th}_{\text{xs}}$  was collected during the same period [19]. It clearly shows that the lack of correlation between the  $^{230}\text{Th}_{\text{xs}}$  content and the lithogenic fraction of the sediment trap material is not restricted to “marginal seas” as previously claimed [10,11,44]. However, it leaves open the possibility that in regions receiving strong lithogenic inputs, lithogenic matter may not scavenge  $^{230}\text{Th}$  as efficiently as in regions with low lithogenic inputs (if it scavenges at all). This is an important observation with regard to the recent debate on the affinity of  $^{230}\text{Th}$  for lithogenic particles [8,10].

#### 4.2. A possible role for $\text{MnO}_2$ in the open ocean

There is no correlation between  $\text{MnO}_2$  and  $^{234}\text{Th}$  (Fig. 4d). This is not surprising because particulate  $^{234}\text{Th}$  in the surface waters is dominated by the scavenging by organic ligands (see previous section) and because photoreduction in surface waters prevents the formation of authigenic  $\text{MnO}_2$  and may dissolve lithogenic  $\text{MnO}_2$  [45]. On the contrary, good correlations are observed between  $^{230}\text{Th}_{\text{xs}}$  and Mn concentrations at 400 m and 1000 m. Unlike the case of the lithogenic fraction, Mn and  $^{230}\text{Th}_{\text{xs}}$  remain correlated even during the high dust event suggesting that Mn could be a significant Th carrier. As noted in Section 3, distinct Mn– $^{230}\text{Th}_{\text{xs}}$  correlations are obtained at 400 m and 1000 m due to the enrichment of  $^{230}\text{Th}_{\text{xs}}$  on marine particles with depth. Lithogenic Mn (estimated with a crustal Mn/ $^{232}\text{Th}$  ratio of 60 g/g) represents from 15% to more than 100% of the total Mn in the POMME samples. In the following discussion, we do not use the distinction between lithogenic and authigenic Mn because the lithogenic Mn is not refractory (at least 30–55% of the lithogenic Mn is readily dissolved at the contact with seawater [46]) and because it is also possible that at least some of the lithogenic Mn present as oxides contribute to Th scavenging. Fe oxides are also known to scavenge Th and they are generally associated to Mn oxides. In the POMME samples, the Fe content is correlated to the lithogenic content. The Fe/Al ratio remains in the range of the lithogenic ma-

terial: Fe/Al=0.40 for the Portuguese margin (this is the upper crust value) and Fe/Al=0.63 for the aerosols from the Sahara [19]. Therefore, it is not possible to calculate a significant authigenic Fe fraction in the POMME samples. However, we cannot rule out that mixed Fe–Mn oxides scavenge Th isotopes on the particles.

The analogy between Cerium (Ce) and  $^{230}\text{Th}_{\text{xs}}$  support that  $\text{MnO}_2$  controls  $^{230}\text{Th}_{\text{xs}}$  [47]. Ce uptake on marine particles is clearly associated to its scavenging on  $\text{MnO}_2$  coatings as Ce (IV) [48,49] or Ce (III) followed by oxidation of Ce (III) to Ce(IV) [47,50]. If a subsequent dissolution of  $\text{MnO}_2$  coatings occurs, Ce(IV) remains bound to the particles. The similarity between Th(IV) and Ce (IV) is confirmed by the much lower solubility of Th and Ce compared to Mn during *in vitro* redissolution of marine particles [51].

While  $\text{MnO}_2$  is known to scavenge efficiently Th isotopes, until now, its involvement was put forward only in very specific environments such as continental margins [52,53], hydrothermal plumes [54], oxic–anoxic transition zone [55]. Conversely, the absence of particulate  $\text{MnO}_2$  in anoxic waters reduces the  $^{230}\text{Th}$  scavenging rate despite a very high flux of particles [55]. If we assume that  $\text{MnO}_2$  is the main Th bearing phase, we can estimate the  $K_{\text{d-MnO}_2}^{\text{Th}}$  required to account for the POMME data. At 1000 m, the dissolved  $^{230}\text{Th}_{\text{xs}}$  content of seawater is of the order of  $5 \times 10^{-15}$  g/l [56] and the  $^{230}\text{Th}_{\text{xs}}/\text{Mn}_{\text{auth}}$  ratio is of the order of  $\sim 1 \times 10^{-7}$  g/g. It yields a  $K_{\text{d-MnO}_2}^{\text{Th}} \approx 2 \times 10^{10}$  ml/g. At 400 m, the dissolved  $^{230}\text{Th}_{\text{xs}}$  content of seawater ( $\sim 3 \times 10^{-15}$  g/l [56]) and the average  $^{230}\text{Th}_{\text{xs}}/\text{Mn}_{\text{auth}}$  ratio of trapped particles ( $\sim 0.75 \times 10^{-7}$  g/g) yield a  $K_{\text{d-MnO}_2}^{\text{Th}}$  value of  $2.5 \times 10^{10}$  ml/g. These results are in remarkable agreement with values calculated in very contrasted marine environments such as ocean margins, marginal sea and open ocean (Table 1). It is also consistent with a gross estimate of  $K_{\text{d-MnO}_2}^{\text{Th}}$  obtained by comparing the  $^{230}\text{Th}$  concentration of Fe–Mn crusts

Table 1  
Partition coefficient of Th between  $\text{MnO}_2$  and seawater

Location	Environment	$K_{\text{d-MnO}_2}^{\text{Th}}$ ( $10^{10}$ ml/g)	References
Northeast Atlantic	Open ocean	2–2.5 <sup>a</sup>	this work
Northeast Atlantic	Open ocean	0.5–1.5 <sup>a</sup>	[5,57]
Mediterranean sea	Enclosed sea	0.4–0.6 <sup>a</sup>	[21]
Equatorial Pacific	Open ocean	3.3	[44]
Guatemala and Panama basins	Coastal ocean	0.1–2 <sup>b</sup>	[52]
Northeast Atlantic	Mn-rich crust	0.5	[58,59]

<sup>a</sup> Estimated with trapped particles.

<sup>b</sup> Estimated with small filtered particles.

and of deep seawater collected nearby. The consistency of the  $K_{d\_MnO_2}^{Th}$  estimates over a large range of oceanic environment contrasts with the lack of general correlation between  $K_{d\_bulk}^{Th}$  and the major components of the sinking particles [60]. Consequently, we infer that  $MnO_2$  could be the main (or at least a significant) host phase of  $^{230}Th$  in the sinking particles throughout the ocean. As noted previously, the role of  $MnO_2$  in the scavenging of Th isotopes and other trace metals is generally accepted at ocean margins where strong Mn inputs occur [52,61]. However, this view was not extended to the open ocean on the premise that  $MnO_2$  does not reach the open ocean [62] and that if it did, there would be no fractionation between  $^{230}Th$  and  $^{231}Pa$  in the open ocean (see below). It is significant that the recent debate on the phase responsible for Th scavenging was based on studies where Mn was not analyzed so that it was not possible to comment on a control of Th flux by  $MnO_2$  and  $MnO_2$  was hardly mentioned [10,11,60,63].

These  $K_{d\_MnO_2}^{Th}$  values are 2 to 4 orders of magnitude higher than the values determined by in vitro experiments [38,64]. These experiments might underestimate the true  $K_{d\_MnO_2}^{Th}$  value because they are conducted with very high  $MnO_2$  concentrations. This underestimate may be due to  $^{230}Th$  bound to colloidal  $MnO_2$  remaining in the “dissolved” phase after filtration of the particulate  $MnO_2$  and/or to the lower specific surface of  $MnO_2$  grains compared to  $MnO_2$  coatings.

A prevalent scavenging of  $^{230}Th$  by  $MnO_2$  would explain several intriguing or problematic features obtained in previous studies: (1) Surprisingly, [8] obtained similar estimates of  $K_{d\_CaCO_3}^{Th}$  and  $K_{d\_litho}^{Th}$ . Although these values could be identical fortuitously, it can be readily understood if the partition of  $^{230}Th_{xs}$  between seawater and particles is not directly controlled by carbonate and lithogenic particles but by  $MnO_2$  coatings disseminated uniformly on carbonate and lithogenic particles. (2) On the other hand, if the lithogenic material is the main phase that scavenges Th, as suggested by [11], there should be very strong variations of  $K_{d\_litho}^{Th}$  between areas receiving large amounts of lithogenic material and remote area receiving only weak aeolian inputs. While the lithogenic particle flux in the open ocean is dominated by the local atmospheric inputs, the Mn particulate flux is not. The residence time of dissolved Mn is long enough to allow advection of dissolved Mn from continental margins and subsequent precipitation on particulate matter [57]. For example, during POMME, authigenic Mn represents between 45% and 85% of the total Mn of the total particulate Mn in the 1000m traps. Thus, the high

value of  $K_{d\_MnO_2}^{Th}$  combined with Mn behaviour in the ocean accounts for the decoupling between lithogenic inputs and  $^{230}Th_{xs}$  scavenging from coastal to open ocean.

At first sight, the  $^{231}Pa$  data seems to contradict the role of  $MnO_2$  as  $^{230}Th$  carrier in the open ocean. Like  $^{230}Th$ ,  $^{231}Pa$  is produced uniformly in the ocean (by radioactive decay of  $^{235}U$ ), its half-life is long compared to its oceanic residence time but it has generally less affinity for marine particles than  $^{230}Th$ . As a consequence, there is usually a strong  $^{230}Th$ – $^{231}Pa$  fractionation in the open ocean with an enrichment of  $^{230}Th$  versus  $^{231}Pa$  in marine particles and a depletion of  $^{230}Th$  versus  $^{231}Pa$  in seawater [5,65]. On the contrary, the lack of  $^{230}Th$ – $^{231}Pa$  fractionation at ocean margins (the so called “boundary scavenging”) is generally attributed to the high flux of  $MnO_2$ -rich particles in these areas because both  $^{230}Th$  and  $^{231}Pa$  are known to have a high affinity for  $MnO_2$  [53,66]. The apparent contradiction is that if  $^{230}Th$  is scavenged by  $MnO_2$  in the ocean and if  $MnO_2$  scavenges  $^{230}Th$  and  $^{231}Pa$  without fractionation, there should be no  $^{230}Th$ – $^{231}Pa$  fractionation in the ocean. However, it was recently proposed that the lack of  $^{231}Pa$ – $^{230}Th$  fractionation at ocean margins could be related to the high diatom production in these areas that enhances  $^{231}Pa$  scavenging compared to open ocean conditions [8]. Alternatively, the lack of  $^{230}Th$ – $^{231}Pa$  fractionation in  $MnO_2$ -rich environment such as continental margins (or hydrothermal plume) could be due to a quantitative scavenging of dissolved  $^{230}Th$  and  $^{231}Pa$  on colloidal  $MnO_2$ . The subsequent aggregation of colloidal  $MnO_2$  on small particles would produce no fractionation between the filtered seawater and the particulate phase. We have already argued that the colloidal  $MnO_2$  could account for the low  $K_{d\_MnO_2}^{Th}$  obtained during in vitro experiments and it appears now that it would also explain the lack of  $^{230}Th$ – $^{231}Pa$  fractionation during these experiments [38,64]. Obviously, analysis of  $^{230}Th$ ,  $^{231}Pa$  and Mn in particulate, colloidal and ultrafiltered solution will be required to confirm or reject the influence of colloidal Mn on  $^{230}Th$ – $^{231}Pa$  fractionation. Should it be rejected, it would leave us with the lithogenic fraction as a possible prevalent Th carrier in the deep water. It would imply very large variations of  $K_{d\_litho}^{Th}$  from one oceanic region to the other. The lack of obvious explanation for these variations has been used to reject the possibility that  $^{230}Th$  scavenging is controlled only by lithogenic particles [63]. In fact, the rather low  $K_{d\_litho}^{Th}$  observed in regions with high lithogenic inputs could arise from the rapid sinking of lithogenic particles through the water column that precludes  $^{230}Th$  scavenging as sug-

gested in Section 4.1. The contribution of this rapidly sinking lithogenic material can be determined because it has a low Mn content as opposed to the Mn-rich and lithogenic-rich particles aggregated to the sinking particles at depth.

#### 4.3. Implications for the particle flux calibration

It clearly appears from the previous discussion that  $^{230}\text{Th}_{\text{xs}}$  in trapped particles is associated with the fine particle aggregated on rapidly sinking particles and that it is most likely adsorbed on  $\text{MnO}_2$  coatings or lithogenic particles. Therefore, trapping efficiencies estimated with  $^{230}\text{Th}_{\text{xs}}$  must be used to correct the vertical flux of elements associated with small particles such as Mn, Ba,  $^{232}\text{Th}$ , REE. On the other hand, the question remains open for POC or  $\text{CaCO}_3$ . A preferential under-trapping of small slowly sinking particles will produce a loss of  $^{230}\text{Th}_{\text{xs}}$  but it will not affect the rapidly sinking aggregates carrying POC and  $\text{CaCO}_3$ . In this case, POC and  $\text{CaCO}_3$  fluxes corrected for trapping efficiency would be overestimated. On the other hand, if small particles are packed in faecal pellets or embedded in large aggregate, the  $^{230}\text{Th}$  calibration will be relevant for POC and  $\text{CaCO}_3$ . Therefore, it is important to determine how efficiently aggregation in the deep-water works. From that point of view, it can be noted that even if carbonates such as foraminifera tests or coccolithophorids do not necessarily directly scavenge Th, they can be coated with Mn oxides [67,68].

Focusing or winnowing of sediments on the sea floor are corrected by normalising the sedimentation rate to the  $^{230}\text{Th}_{\text{xs}}$  inventory in sediments [69]. Again, particle fractionation during sediment redistribution could put limits on the use of the Th-normalisation method and could yield an overestimation of large particle redistribution based on  $^{230}\text{Th}$  inventory. Combinations of thorium isotopes are potentially powerful tracers of particle aggregation and disaggregation [70]. However, such application is based on the assumption that in situ-produced Th isotopes are carried by the same phases (or at least the same particles). The strong decoupling observed between  $^{230}\text{Th}$  and  $^{234}\text{Th}$  in this study implies that Th isotopes must be used cautiously to calibrate particle dynamic models.

The implications of this work extend beyond the carbon export. With the development of MC-ICP-MS, it is possible to obtain very detailed water column  $^{230}\text{Th}$  and  $^{231}\text{Pa}$  profiles that bare information on the thermohaline-circulation [71]. As the deep currents are estimated through the difference between in situ production and particulate transport of  $^{230}\text{Th}$  [72], it is necessary to

have well constrained  $^{230}\text{Th}$  particulate fluxes at the basin scales. The control of Th scavenging by Mn oxides rather than by carbonates or lithogenic material could change the detailed pattern of Th scavenging over the ocean and hence the estimation of the deep currents. The  $^{230}\text{Th}$ – $^{231}\text{Pa}$  pair in sediments is also used to constrain both paleo-ventilation and paleo-particle fluxes [62]. Here again, determination of the host phase(s) of these nuclides is a prerequisite for a reliable use of these proxies. A substantial  $^{230}\text{Th}$ – $^{231}\text{Pa}$  fractionation by  $\text{MnO}_2$  would help to match the past variation of the  $^{230}\text{Th}/^{231}\text{Pa}$  recorded in sediments and paleoparticle fluxes in the Pacific ocean [73].

## 5. Conclusion

Recently, the question of  $^{230}\text{Th}$  and  $^{231}\text{Pa}$  scavenging in the deep ocean has been studied through the relationships of these nuclides with the major components of the sinking particles. In the present study, the comparison of  $^{230}\text{Th}$  with an extended set of geochemical tracers somewhat changes the perspective. First, we clearly show that  $^{230}\text{Th}$  and  $^{234}\text{Th}$  are not controlled by the same phases owing to their different depths of scavenging: while  $^{234}\text{Th}$  is associated with the organic matter recently produced in the surface water,  $^{230}\text{Th}_{\text{xs}}$  is mostly associated with the fine suspended particles that are aggregated to the large sinking particles throughout the water column. Second, we raise the possibility that  $^{230}\text{Th}_{\text{xs}}$  in the deep ocean is not controlled by major phases but rather by  $\text{MnO}_2$  coatings. While further testing of this hypothesis is required, it stresses that  $^{230}\text{Th}$  (as well as  $^{231}\text{Pa}$ ) scavenging cannot be studied just through the correlations of  $^{230}\text{Th}_{\text{xs}}$  with the major phases in the trapped material.

## Acknowledgements

We thank L. Memery and G. Reverdin, PIs of the POMME Program, the Captains and crews of the R/V *L'Atalante* and R/V *Thalassa* and the Chief Scientists of the cruises. C. Marec, A. Dubreule and L. Scoarnec, who allowed bucketful use of the traps, are greatly acknowledged. We are grateful to C. Guieu for her efficient management of the sediment trap team “cellule piège” of CNRS/INSU. J. Mosseri, K. Leblanc and B. Queguiner kindly provided bSi data. We thank N. Frank for his support with the TIMS at LSCE. We are grateful to F. Candaudap for his help with the Elan 6000 utilization. The constructive comments of 2 anonymous reviewers were very much appreciated. The POMME Program was supported

by the French agencies CNRS/ INSU (PROOF-PATOM), Ifremer, Meteo-France and SHOM.

## Appendix A. Supplementary data

Supplementary data associated with this article can be found, in the online version, at [doi:10.1016/j.epsl.2005.09.059](https://doi.org/10.1016/j.epsl.2005.09.059).

## References

- [1] W.D. Gardner, Sediment trap dynamics and calibration: a laboratory evaluation, *J. Mar. Res.* 38 (1980) 17–39.
- [2] M.P. Bacon, C.-H. Huh, A.P. Fleer, W.G. Deuser, Seasonality in the flux of natural radionuclides and plutonium in the deep Sargasso Sea, *Deep-Sea Res.* 32 (1985) 273–286.
- [3] K.O. Buesseler, Do upper-ocean sediment traps provide an accurate record of particle flux? *Nature* 353 (1991) 420–423.
- [4] M.P. Bacon, R.F. Anderson, Distribution of thorium isotopes between dissolved and particulate forms in the Deep-Sea, *J. Geophys. Res.* 87 (1982) 2045–2056.
- [5] J.C. Scholten, J. Fietzke, S. Vogler, M.M. Rutgers van der Loeff, A. Mangini, W. Koeve, J. Wanick, P. Stoffers, A. Antia, J. Kuss, Trapping efficiencies of sediment traps from the deep Eastern North Atlantic: the  $^{230}\text{Th}$  calibration, *Deep-Sea Res., Part 2, Top. Stud. Oceanogr.* 48 (2001) 2383–2408.
- [6] K.O. Buesseler, M. Bacon, J.K. Cochran, H.D. Livingston, Carbon and nitrogen export during the JGOFS North Atlantic Bloom Experiment estimated from  $^{234}\text{Th}$ / $^{238}\text{U}$  disequilibrium, *Deep-Sea Res.* 39 (1992) 1115–1137.
- [7] E.-F. Yu, R. Francois, M.P. Bacon, S. Honjo, A.P. Fleer, S.J. Manganini, M.M. Rutgers van der Loeff, V. Ittekkot, Trapping efficiency of bottom-tethered sediment traps estimated from the intercepted fluxes of  $^{230}\text{Th}$  and  $^{231}\text{Pa}$ , *Deep-Sea Res., Part 1, Oceanogr. Res. Pap.* 48 (2001) 865–889.
- [8] Z. Chase, R.F. Anderson, M.Q. Fleisher, P.W. Kubik, The influence of particle composition and particle flux on scavenging of Th, Pa and Be in the ocean, *Earth Planet. Sci. Lett.* 204 (2002) 215–229.
- [9] H. Narita, R. Abe, K. Tate, Y. Kim, K. Harada, S. Tsunogai, Anomalous large scavenging of  $^{230}\text{Th}$  and  $^{231}\text{Pa}$  controlled by particle composition in the northwestern North Pacific, *J. Oceanogr.* 59 (2003).
- [10] S. Luo, T.-L. Ku, Reply to Comment on “On the importance of opal, carbonate, and lithogenic clays in scavenging and fractionating  $^{230}\text{Th}$ ,  $^{231}\text{Pa}$  and  $^{10}\text{Be}$  in the ocean”, *Earth Planet. Sci. Lett.* 220 (2004) 223–229.
- [11] S. Luo, T.-L. Ku, On the importance of opal, carbonate and lithogenic clays in scavenging and fractionating  $^{230}\text{Th}$ ,  $^{231}\text{Pa}$  and  $^{10}\text{Be}$  in the ocean, *Earth Planet. Sci. Lett.* 220 (2004) 201–211.
- [12] S.M. Trimble, M. Baskarana, D. Porcelli, Scavenging of thorium isotopes in the Canada Basin of the Arctic Ocean, *Earth Planet. Sci. Lett.* 222 (2004) 915–932.
- [13] H.N. Edmonds, S.B. Moran, J.A. Hoff, R.L. Edwards, J.N. Smith, Protactinium-231 and thorium-230 abundances and high scavenging rates in the Western Arctic Ocean, *Science* 280 (1998) 405–407.
- [14] H.N. Edmonds, S.B. Moran, H. Cheng, R.L. Edwards,  $^{230}\text{Th}$  and  $^{231}\text{Pa}$  in the Arctic Ocean: implications for particle fluxes and basin-scale Th/Pa fractionation, *Earth Planet. Sci. Lett.* 227 (2004) 155–167.
- [15] M.S. Quigley, P.H. Santschi, L. Guo, B.D. Honeyman, Sorption irreversibility and coagulation behavior of  $^{234}\text{Th}$  with marine organic matter, *Mar. Chem.* 76 (2001) 27–45.
- [16] M. Baskaran, P.W. Swarzenski, D. Porcelli, Role of colloidal material in the removal of  $^{234}\text{Th}$  in the Canada Basin of the Arctic Ocean, *Deep-Sea Res.* 50 (2004) 1353–1373.
- [17] L. Mémary, G. Reverdin, J. Paillet, A. Oeschies, Introduction to the POMME special section: Thermocline ventilation and biogeochemical tracer distribution in the northeast Atlantic Ocean and impact of mesoscale dynamics, *J. Geophys. Res.* 110 (in press) C07S01, [doi:10.1029/2005JC002976](https://doi.org/10.1029/2005JC002976).
- [18] M. Goutx, C. Guigou, N. Leblond, A. Desnues, A. Dufour, D. Aritio, C. Guieu, Particle flux in the North–East Atlantic Ocean during the POMME experiment (2001): Results from mass, carbon, nitrogen and lipid biomarkers from the drifting sediment traps, *J. Geophys. Res.* 110 (in press) C07S20, [doi:10.1029/2004JC002749](https://doi.org/10.1029/2004JC002749).
- [19] C. Guieu, M. Roy-Barman, N. Leblond, C. Jeandel, M. Souhaut, B. Le Cann, A. Dufour, C. Bournot, Vertical particle flux in the northeast Atlantic Ocean (POMME experiment), *J. Geophys. Res.* 110 (in press) C07S18, [doi:10.1029/2004JC002672](https://doi.org/10.1029/2004JC002672).
- [20] M. Roy-Barman, J.H. Chen, G.J. Wasserburg,  $^{230}\text{Th}$ – $^{232}\text{Th}$  systematics in the Central Pacific Ocean: the sources and the fates of thorium, *Earth Planet. Sci. Lett.* 139 (1996) 351–363.
- [21] M. Roy-Barman, L. Coppola, M. Souhaut, Thorium isotopes in the Western Mediterranean Sea: an insight into the marine particle dynamics, *Earth Planet. Sci. Lett.* 196 (2002) 161–174.
- [22] M.M. Rutgers van der Loeff, W.S. Moore, Determination of natural radio active tracers, in: M.E.K. Grasshoff, K. Kremling (Eds.), *Methods of Seawater Analysis*, Chapter 13, Verlag Chemie, 1999, pp. 365–397.
- [23] P.G. Brewer, Y. Nozaki, D.W. Spencer, A.P. Fleer, Sediment trap experiments in the deep North Atlantic: isotopic and elemental fluxes, *J. Mar. Res.* 38 (1980) 703–728.
- [24] S.R. Taylor, S.M. McLennan, *The Continental Crust: Its Composition and Evolution*, Blackwell Scientific, Oxford, 1985, p. 46.
- [25] R.A. Mortlock, P.N. Froelich, A simple method for the rapid determination of biogenic opal in pelagic marine sediments, *Deep-Sea Res.* 36 (1989) 1415–1426.
- [26] J. Mosseri, B. Quéguiner, P. Rimmelin, N. Leblond, C. Guieu, Silica fluxes in the northeast Atlantic frontal zone of Mode Water formation (38–45°N, 16–22°W) in 2001–2002, *J. Geophys. Res.* 110 (in press) C07S19, [doi:10.1029/2004JC002615](https://doi.org/10.1029/2004JC002615).
- [27] K. Leblanc, A. Leynaert, C. Fernandez I, P. Rimmelin, T. Moutin, P. Raimbault, J. Ras, B. Quéguiner, A seasonal study of diatom dynamics in the North Atlantic during the POMME experiment (2001): evidence for Si limitation of the spring bloom, *J. Geophys. Res.* (2005) 110, [doi:10.1029/2004JC002621](https://doi.org/10.1029/2004JC002621) (C07S14).
- [28] P.S. Andersson, G.J. Wasserburg, J.H. Chen, D.A. Papanastassiou, J. Ingri,  $^{238}\text{U}$ – $^{234}\text{U}$  and  $^{232}\text{Th}$ – $^{230}\text{Th}$  in the Baltic sea and in river water, *Earth Planet. Sci. Lett.* 130 (1995) 217–234.
- [29] Y. Nozaki, H.-S. Yang, M. Yamada, Scavenging of Thorium in the ocean, *J. Geophys. Res.* 92 (1987) 772–778.
- [30] F. Dehairs, D. Shopova, S. Ober, C. Veth, L. Goeyens, Particulate barium stocks and oxygen consumption in the Southern Ocean mesopelagic water column during spring and early summer: relationship with export production, *Deep-Sea Res., Part 2, Top. Stud. Oceanogr.* 44 (1997) 497–516.

- [31] E. Robin, C. Rabouille, G. Martinez, I. Lefevre, J.L. Reyss, P. Van Beek, C. Jeandel, Direct barite determination using SEM/EDS-ACC system: implication for constraining barium carriers and barite preservation in marine sediments, *Mar. Chem.* 82 (2003) 289–306.
- [32] D.W. Lea, E. Boyle, Barium in planktonic foraminifera, *Geochim. Cosmochim. Acta* 55 (1991) 3321–3333.
- [33] P. van Beek, J.-L. Reyss, Ra in marine barite: new constraints on supported  $^{226}\text{Ra}$ , *Earth Planet. Sci. Lett.* 187 (2001) 147–161.
- [34] C. Beucher, P. Tréguer, A.-M. Hapette, R. Corvaisier, N. Metz, J.-J. Pichon, Intense summer Si-recycling in the surface Southern Ocean, *Geophys. Res. Lett.* 31 (2004) L09305, doi:10.1029/2003GL018998.
- [35] P. Tréguer, D.M. Nelson, S. Gueneley, C. Zeyons, J. Morvan, A. Buma, The distribution of biogenic and lithogenic silica and the composition of particulate organic matter in the Scotia Sea and the Drake Passage during autumn 1987, *Deep-Sea Res., Part 1, Oceanogr. Res. Pap.* 37 (1990) 833–851.
- [36] J.K. Bishop, D.R. Ketten, J.M. Edmond, The chemistry, biology and vertical flux of particulate matter from the upper 400 m of the Cape basin in the southeast Atlantic ocean, *Deep-Sea Res., Part 1, Oceanogr. Res. Pap.* 25 (1978) 1121–1161.
- [37] L.F. Robinson, N.S. Belshaw, G.M. Henderson, U and Th isotopes in seawater and modern carbonates from the Bahamas, *Geochim. Cosmochim. Acta* 68 (2004) 1777–1789.
- [38] W. Geibert, R. Usbeck, Adsorption of thorium and protactinium onto different particle types: experimental findings, *Geochim. Cosmochim. Acta* 68 (2004) 1489–1501.
- [39] L. Coppola, M. Roy-Barman, P. Wassmann, S. Mulsow, J. Jeandel, Calibration of sediment traps and particulate organic carbon export using  $^{234}\text{Th}$  in the Barents Sea, *Mar. Chem.* 80 (2002) 11–26.
- [40] L. Coppola, M. Roy-Barman, S. Mulsow, P. Povinec, C. Jeandel, Low particulate organic carbon export in the frontal zone of the Southern Ocean (Indian sector) revealed by  $^{234}\text{Th}$ , *Deep-Sea Res., Part 1, Oceanogr. Res. Pap.* 52 (2005) 52.
- [41] K. Hirose, E. Tanoue, The vertical distribution of the strong ligand in particulate organic matter in the North Pacific, *Mar. Chem.* 59 (1998) 235–252.
- [42] R.J. Murnane, J.K. Cochran, J.L. Sarmiento, Estimate of particle- and thorium-cycling rates in the northwest Atlantic Ocean, *J. Geophys. Res.* 99 (1994) 3373–3392.
- [43] D.K. Rea, The paleoclimatic record provided by eolian deposition in the deep sea—The geologic history of wind, *Rev. Geophys.* 32 (1994) 159–195.
- [44] S. Luo, T.-L. Ku, Oceanic  $^{231}\text{Pa}/^{230}\text{Th}$  ratio influenced by particle composition and remineralisation, *Earth Planet. Sci. Lett.* 167 (1999) 183–195.
- [45] W.G. Sunda, S. Huntsman, G.R. Harvey, Photoreduction of manganese oxides in seawater and its geochemical and biological implications, *Nature* 301 (1983) 234–236.
- [46] C. Guieu, R.A. Duce, R. Arimoto, Dissolved input of Manganese in the ocean: the aerosol source, *J. Geophys. Res.* 99 (1994) 18789–18800.
- [47] D.S. Alibo, Y. Nozaki, Rare earth elements in seawater: Particle association, shale-normalization, and Ce oxidation, *Geochim. Cosmochim. Acta* (1999) 363–372.
- [48] J.W. Moffett, Microbially mediated cerium oxidation in sea water, *Nature* 345 (1990) 421–423.
- [49] E.R. Sholkovitz, W.M. Landing, B.L. Lewis, Ocean particle chemistry: the fractionation of rare earth elements between suspended particles and seawater, *Geochim. Cosmochim. Acta* 58 (1994) 1567–1579.
- [50] K. Tachikawa, C. Jeandel, A. Vangriesheim, B. Dupré, Distribution of rare earth elements and neodymium isotopes in suspended particles of the tropical Atlantic Ocean (EUMELI site), *Deep-Sea Res.* 46 (1999) 733–756.
- [51] R. Arraes-Mescoff, L. Coppola, M. Roy-Barman, M. Souhaut, K. Tachikawa, C. Jeandel, R. Sempéré, C. Yoro, The behavior of Al, Mn, Ba, Sr, REE and Th isotopes during in vitro bacterial degradation of large marine particles, *Mar. Chem.* 73 (2001) 1–19.
- [52] R.F. Anderson, M.P. Bacon, P.G. Brewer, Removal of  $^{230}\text{Th}$  and  $^{231}\text{Pa}$  at ocean margins, *Earth Planet. Sci. Lett.* 66 (1983) 73–90.
- [53] G.B. Shimmield, J.W. Murray, J. Thomson, M.P. Bacon, R.F. Anderson, N.B. Price, The distribution and behaviour of  $^{230}\text{Th}$  and  $^{231}\text{Pa}$  at an ocean margin, Baja California, Mexico, *Geochim. Cosmochim. Acta* 50 (1986) 2499–2507.
- [54] G.B. Shimmield, N.B. Price, The scavenging of U,  $^{230}\text{Th}$ , and  $^{231}\text{Pa}$  during pulsed hydrothermal activity at  $20^\circ\text{S}$ , East Pacific Rise, *Geochim. Cosmochim. Acta* 52 (1988) 669–677.
- [55] C.-A. Huh, J.M. Kelley, J.W. Murray, C.L. Wei, Water column distribution of  $^{230}\text{Th}$  and  $^{232}\text{Th}$  in the Black Sea, *Deep Sea Res.* 41 (1994) 101–112.
- [56] M. Roy-Barman, R. El Hayek, I. Voegelé, M. Souhaut, N. Leblond, C. Jeandel, Constraining the seasonal particle flux in the eastern North Atlantic with Thorium isotopes, EUG-AGU Meeting Nice (Abstract), 2003.
- [57] J. Kuss, K. Kremling, Particulate trace element fluxes in the deep northeast Atlantic Ocean, *Deep-Sea Res., Part 1, Oceanogr. Res. Pap.* 46 (1999) 1377–1403.
- [58] C. Claude-Ivanaj, A.W. Hofmann, I. Vlastélic, A. Koschinsky, Recording changes in ENADW composition over the last 340 ka using high-precision lead isotopes in a Fe–Mn crust, *Earth Planet. Sci. Lett.* 188 (2001) 73–89.
- [59] A. Mangini, R.M. Key, A  $^{230}\text{Th}$  profile in the Atlantic Ocean, *Earth Planet. Sci. Lett.* 62 (1983) 377–384.
- [60] J.C. Scholten, J. Fietzke, A. Mangini, P. Stoffers, T. Rixen, B. Gaye-Haake, T. Blanze, V. Ramaswamy, F. Sirocko, H. Schulz, V. Ittekkot, Radionuclide fluxes in the Arabian Sea: the role of particle composition, *Earth Planet. Sci. Lett.* 230 (2005) 319–337.
- [61] D.W. Spencer, M.P. Bacon, P.G. Brewer, Models of the distribution of  $^{210}\text{Pb}$  in a section across the North Equatorial Atlantic Ocean, *J. Mar. Res.* 39 (1981) 119–137.
- [62] G. Henderson, R.F. Anderson, The U-series toolbox for paleoceanography, in: B. Bourdon (Ed.), *Uranium-Series Geochemistry, Reviews in Mineralogy and Geochemistry*, vol. 52, 2003, pp. 493–531, e.a. eds.
- [63] Z. Chase, R.F. Anderson, Comment on “On the importance of opal, carbonate, and lithogenic clays in scavenging and fractionating  $^{230}\text{Th}$ ,  $^{231}\text{Pa}$  and  $^{10}\text{Be}$  in the ocean” by S. Luo and T.-L. Ku, *Earth Planet. Sci. Lett.* 220 (2004) 213–222.
- [64] L. Guo, M. Chen, C. Gueguen, Control of Pa/Th ratio by particulate chemical composition in the ocean, *Geophys. Res. Lett.* 29 (2002) 1961.
- [65] S.B. Moran, C.-C. Shen, H.N. Edmonds, S.E. Weinstein, J.N. Smith, R.L. Edwards, Dissolved and particulate  $^{231}\text{Pa}$  and  $^{230}\text{Th}$  in the Atlantic Ocean: constraints on intermediate/deep water age, boundary scavenging, and  $^{231}\text{Pa}/^{230}\text{Th}$  fractionation, *Earth Planet. Sci. Lett.* 203 (2002) 999–1014.
- [66] R.F. Anderson, M.Q. Fleisher, P.E. Biscaye, N. Kumar, B. Ditrich, P. Kubik, M. Suter, Anomalous boundary scavenging

- in the Middle Atlantic Bight: evidence from  $^{230}\text{Th}$ ,  $^{231}\text{Pa}$ ,  $^{10}\text{Be}$  and  $^{210}\text{Pb}$ , *Deep-Sea Res., Part 2, Top. Stud. Oceanogr.* 41 (1994) 537–561.
- [67] J.H. Martin, G.A. Knauer, Vertex: Manganese transport with  $\text{CaCO}_3$ , *Deep-Sea Res.* 30 (1983) 411–425.
- [68] D. Vance, A.E. Scrivner, P. Beney, M. Staubwasser, G.M. Henderson, N.C. Slowey, The use of foraminifera as a record of the past neodymium isotope composition of seawater, *Paleoceanography* 19 (2004) PA2009, doi:10.1029/2003PA000957.
- [69] R. Francois, M. Frank, M.M. Rutgers van der Loeff, M.P. Bacon,  $^{230}\text{Th}$  normalization: An essential tool for interpreting sedimentary fluxes during the late Quaternary, *Paleoceanography* 19 (2004) PA1018, doi:10.1029/2003PA000939.
- [70] S.L. Clegg, M. Withfield, A generalized model for the scavenging of trace metals in the open ocean: II. Thorium scavenging, *Deep Sea Res.* 38 (1991) 91–120.
- [71] M.S. Choi, R. Francois, K. Sims, M.P. Bacon, S. Brown-Leger, A.P. Flerer, L. Ball, D. Schneider, S. Pichat, Rapid determination of  $^{230}\text{Th}$  and  $^{231}\text{Pa}$  in seawater by desolvated micro-nebulisation Inductively Coupled Mass Spectrometry, *Mar. Chem.* 76 (2001) 99–112.
- [72] G.M. Henderson, C. Heinze, R.F. Anderson, A.M.E. Winguth, Global distribution of the  $^{230}\text{Th}$  flux to ocean sediments constrained by GCM modelling, *Deep-Sea Res., Part 1, Oceanogr. Res. Pap.* 46 (1999) 1861–1893.
- [73] S. Pichat, K.W.W. Sims, R. François, J.F. McManus, S. Brown Leger, F. Albarède, Lower export production during glacial periods in the equatorial Pacific derived from  $(^{231}\text{Pa}/^{230}\text{Th})_{\text{xs},0}$  measurements in deep-sea sediments, *Paleoceanography* 19 (2004) PA4023, doi:10.1029/2003PA000994.